5-23-2010

The Pyridine-Formic Acid Interaction: A Matrix Isolation and Polymer Soft Landing Study

Jeffrey Michael Rodgers
Dickinson College

The Pyridine-Formic Acid Interaction: A Matrix Isolation and Polymer Soft Landing Study

By
Jeffrey M. Rodgers

Submitted in partial fulfillment of the Honors Requirements
for the Department of Chemistry

Dr. Cindy Samet, Supervisor
Dr. R. David Crouch, Reader
Dr. Pamela J. Higgins, Reader
Dr. Michael S. Holden, Reader
Dr. Kristi J. Humphreys, Reader
Dr. Sarah K. St. Angelo, Reader
Dr. Amy E. Witter, Reader

May 3 2010

Abstract

The hydrogen-bonded complex of formic acid and pyridine has been characterized for the first time through isolation in argon matrices at 16 K, both via traditional matrix isolation experiments and by soft landing of formic acid on poly(4-vinylpyridine) (PVP). The formation of the formic acid-PVP complex was confirmed by the distinct red shifts of both the O-H and C=O stretching modes (~400 cm^{-1} and ~20 cm^{-1}, respectively) and the blue shift of the C-O stretching mode (~130 cm^{-1}) in the infrared spectrum. The shifts indicative of hydrogen bonding are similar in this soft landing experiment, and this represents a novel example of the characterization of hydrogen bonding in polymers through Fourier transform infrared absorption spectroscopy. These results were analyzed by direct comparison to a standard matrix isolation experiment with pyridine and formic acid. To support and confirm these experimental results, density functional theory calculations were employed to obtain an optimized geometry, theoretical infrared absorption bands, and binding energies for pyridine and PVP in complexes with formic acid. Values of 10.9 and 11.3 kcal/mol were obtained for the binding energy for a pyridine-formic acid bond and PVP-formic acid bond, respectively.

Introduction

Matrix isolation has been used for over a century as a method of studying specific interactions of atoms and molecules.[1] Dilute gaseous mixture of samples to be investigated (guest) are prepared in an inert gas such as argon (host) and are solidified at temperatures far below the freezing point of the host and studied through spectroscopy. Studying the guest molecules in an isolated state can provide information about a chemical interaction than a reaction of bulk substances in the liquid or gaseous phase. When several different guest molecules are present, they can form complexes or react while isolated in the host, and chemical changes are observable through changes in their infrared spectra. Previously, matrix isolation studies have been undertaken to explore interactions of interest in other fields of chemistry, for example, the investigation of potential environmentally hazardous atmospheric complexes. Molecules such as

hydrochlorofluorocarbons (HCFCs), initially considered appropriate alternatives to chlorofluorocarbons (CFCs), have been studied using matrix isolation to confirm their contribution to climate change as greenhouse gases.[2] Matrix isolation has recently allowed for the first ever observation of several intermediates in the ozonolysis reaction through the codepostion of ozone and 2-butene in an argon matrix.[3] Chemists have looked to the matrix isolation community for detailed studies of systems in order to fully characterize their structure, reactivity, and/or function.

Hydrogen bonding is an important and fundamental force that occurs both within molecules (intramolecular) and between molecules (intermolecular) in which there is an electronegative element interacting with a hydrogen atom. In a conventional hydrogen bond, the hydrogen atom must be attached to a nitrogen, oxygen, or fluorine. In proteins, DNA, and many other naturally occurring systems, hydrogen bonding is the primary directing force in the determination of structure and function. Hydrogen bonding is also involved in the formation of self-assembled monolayers and other nanostructures. A conventional hydrogen bond is known to occur between the nitrogen of pyridine and the acidic hydrogen of formic acid (Figure 1a). Additionally, poly(4-vinylpyridine) (PVP) (Figure 1b), a polymer containing chains of carbon with pyridyl groups attached, also exhibits hydrogen bonding capabilities.

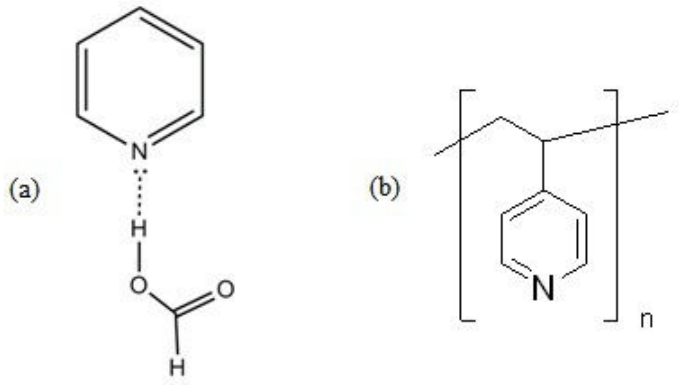

Figure 1: (a) Optimal geometry of pyridine-formic acid interaction: coplanar. Figure adapted from calculated geometry by Fernandez-Berridi et al. using Density Functional Theory (b) Diagram of poly(4-vinylpyridine). For the polymer used in this experiment, each polymer chain consisted of ~1500 pyridine units (i.e. $n \approx 1500$).

Matrix isolation is an excellent tool for examining hydrogen bonded complexes and has previously been utilized to demonstrate even very weakly bound complexes. Because of the extremely low temperatures reached in these experiments, even highly unstable or weak complexes can be studied due to diminished entropic limitations;[4] even systems experiencing a "non-traditional" C-H···N hydrogen bond have been characterized using matrix isolation.[5,6] The coupling of matrix isolation apparatus with an infrared spectrometer allows for the detection of spectral changes indicative of a hydrogen bonding interaction. The technique relies heavily on the comparison of parent spectra with the complex spectra obtained through matrix isolation or soft landing. Generally, the presence of a hydrogen bond manifests as a new absorption not present in the parent spectra or an intensification or broadening of an existing mode. This perturbation of parent absorption frequencies is caused by an atom associated with the vibrating bond being influenced by the electrostatic interaction. Additionally, the movement of electron density toward the electronegative element participating in a hydrogen bond can incite spectral changes in other parts of the molecule;[7] for example, in pyridine the π-electron density shifts heavily toward nitrogen when it forms a hydrogen bond and can lead to changes in C-H shifts elsewhere in the molecule. In both matrix isolation and soft landing studies, these perturbations, shifts, or other changes in the spectra can possibly be observed by direct spectral comparison. However, when new bands are particularly weakly absorbing or are in close proximity to many parent modes, subtraction of the parent spectrum from the codeposition or soft landing spectra is necessary to visualize and pinpoint their location.[8]

Additionally, hydrogen bonding interactions have been probed using the matrix isolation technique with applications in biochemistry, but very complex molecules, potentially involving multiple hydrogen bonding sites, are often involved in such studies, leading to difficulties in spectral assignment. In recent years, hydrogen bonding has become extremely important in the field of nanochemistry, particularly regarding interactions in layered thin films.[9] If a nanostructure's formation and function is dependent on hydrogen bonding, key physical information is desirable including the optimal geometry of the molecules and strength of the bond

formed. In particular, hydrogen bonding in thin films remains a highly researched and debated field. Several groups have studied the interlayer forces between PVP and poly(acrylic acid) (PAA) with differing results, some reporting the presence of hydrogen bonding,[10,11] while others have reported evidence of charged carboxyl groups–evidence of a proton transfer reaction.[12] PVP and PAA have also been used in the self-assembly of CdSe nanoparticles into monolayers driven by intermolecular attractions,[9] so PVP stands out as a universal model system for hydrogen bonding in polymers. Because the interlayer forces between PVP and PAA are not fully understood, the soft landing of formic acid on PVP and its direct comparison to the matrix isolation of pyridine and formic acid is essential to characterize the interaction as a hydrogen bond. Thus, a new task has been presented to the matrix isolation community–characterization of the forces fundamental to thin films.

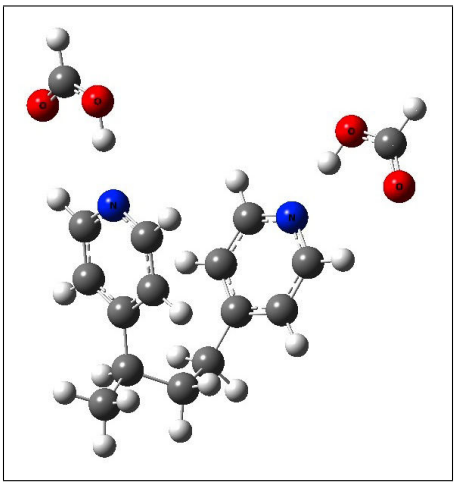

Figure 2: Structure of PVP dimer and 2 molecules of formic acid as calculated by DFT.

A slightly modified version of matrix isolation called soft landing has been used to study thin films of polymers with hydrogen bond acceptors. Unlike with matrix experiments, instead of depositing two different guest molecules simultaneously, a thin polymer film is first placed on the matrix window and a rare gas mixture one or more reactants is "soft-landed" onto the polymer. A recent application focused on the infrared reflectance spectrum and thermal decomposition of vanadium-benzene sandwich compounds after soft landing on an organic polymer surface.[13] To date, this technique has never been used to study hydrogen-bonding

in polymers with FT-IR absorbance due to issues involving low signal. In standard matrix isolation experiments, product is formed continuously as the guest/host mixtures are deposited. The Beer-Lambert Law (given in Equation 1)

$$A = \varepsilon bc \tag{1}$$

gives the relationship between absorbance A at a particular wavelength where ε is the molar absorptivity at that wavelength, b is the cell length (thickness of the rare gas matrix in the case of this study) and c is the concentration of the absorbing species. In the case of a matrix isolation experiment, the matrix thickness b and concentration of complex c both continually increase throughout the deposition. In a soft landing experiment, however, the sites available for hydrogen bonding on the thin film are limited, and the complex concentration does not increase constantly as the reaction proceeds. Furthermore, the matrix thickness b does continue to increase, resulting in smaller absorbance values for complexes formed during a soft landing experiment. Only a cross section of the matrix in direct contact with the thin film-coated window will contain complexes exhibiting hydrogen bonding activity.

Computational chemistry has become increasingly common and integral to the study of hydrogen bonded systems. Density functional theory (DFT) allows for the accurate determination of the optimized structure, energy, and calculated infrared spectra of chemistry systems. By modeling the parent molecules individually and the complex, the binding energy contributed by the hydrogen bond can be determined. Furthermore, the predicted infrared spectrum of the complex indicates the expected infrared band shifts associated with the hydrogen bond. Since matrix isolation creates an idealized environment in which to characterize a hydrogen-bonded complex (low temperature, diminished intermolecular forces, no solvent interactions) experimental infrared absorption bands can be directly compared with those calculated using DFT.

This study characterizes the model hydrogen bonding interaction between formic acid and pyridine using a comparison of the matrix isolation and soft landing experimental spectra

combined with the theoretical predictions of density functional theory. The polymer PVP is known to exhibit hydrogen bonding properties, but soft landing onto thin films has never before been utilized to study hydrogen bonding via FT-IR absorbance spectroscopy. PVP represents a universal model as a polymer onto which acidic species can be landed, and it is important to fully understand the interaction that occurs between formic acid and PVP and whether it is an appropriate analog for that of formic acid and pyridine. The spectral changes indicative of hydrogen bonding activity were present both in the soft landing of formic acid onto PVP and in the matrix isolation of formic acid and pyridine, and thus this work yields a valuable result which may be applied in the characterization of many other hydrogen bonding systems.

Experimental Section

All soft landing experiment and matrix isolation experiments were carried out using the same equipment. A stainless steel vacuum system with Nupro Teflon-seat high-vacuum valves was used for gas handling. Pumping was accomplished with a Model 1400B Welch roughing pump and a Varian V-301 Turbomolecular pump. Vacuums on the order of 10^{-7} Torr at the gauge (cold cathode, Varian) were obtained. Cryogenics were handled by a model 8220 closed cycle helium circulator (CTI, Inc.), operating at temperatures down to 10 K. Gaseous samples were prepared in 2 L stainless steel cans and deposited using precise needle valves onto the cold spectrometer window mounted with indium in a copper window holder on the second stage of the CTI, Inc. cold head. The temperature of the window was monitored and regulated using a RMC-Cryosystems model 4025 digital cryogenic temperature controller. The steel vacuum container connected to the cold head was equipped with KBr outer windows and situated in the sample beam of a Thermo Nicolet Nexus 870 FT-IR spectrometer.

Formic acid (98+%, pure, Acros) and pyridine (min. 99.8%, EMD) were first used without further purification and were introduced into the stainless sample cans using a freeze-pump-thaw cycle at 77 K. Due to the hygroscopic properties of formic acid, water infrared absorption peaks appeared when a sample was prepared using the same reagent several months

after it was opened. Drying and distillation of the formic acid was necessary and was first attempted using molecular sieves (3Å, Fluka). The formic acid reacted with these molecular sieves, resulting in a contaminating residue. Therefore, the formic acid was dried using boric anhydride and distilled at 101°C before being used for any additional samples.[14] Argon (Matheson) was used without further purification as the host matrix gas for all experiments. These samples were deposited at rates ranging from $0.5 - 2.0$ mmol/h, for times ranging from 8-24 hours at 16 K. Infrared scans were recorded at 0.25, 0.50, and 1.0 cm^{-1} resolutions. Certain samples were annealed after deposition to 30 K and recooled to 16 K before final spectra were collected. Experimental details varied between the soft landing and matrix isolation experiments.

Soft Landing Experiments. In the soft landing of formic acid on a thin film of PVP, a formic acid/argon mixture was deposited by a single jet on a thin film-coated CaF_2 window. First, a 1%w/v solution of PVP (typical $M_w = 160,000$, Sigma-Aldrich) was prepared in ethanol (200 proof). The thin film was placed on the deposition window by slowly adding 1% PVP solution with a pipette until a raised droplet covered the surface. As the solvent evaporated, the polymer was left as a translucent film. This process was attempted and modified multiple times to achieve the desired film; initial attempts were unsuccessful when the droplet size was too small, resulting in an opaque film. A 1% solution resulted in the desired thickness and translucency, and increasing the concentration did not result in more available hydrogen bonding sites. This value is consistent with Malynych et al. who reported that the PVP surface morphology is not dependent on concentration between 0.01% and 3%.[15] It was necessary to use a CaF_2 for this preparation as it does not interact adversely with ethanol; a standard KBr matrix isolation window could not be used because it would absorb ethanol during this evaporation process, interfering with infrared spectra collection. The PVP thin film infrared spectrum was in strong agreement with Cesteros et al..[16] Background spectra for soft landing experiments were obtained with the thin film in place, and thus the PVP parent infrared absorption bands are not observed in these experiments.

Matrix Isolation Experiments. To obtain matrix isolation spectra for comparison, samples of formic acid and pyridine in argon were deposited in twin-jet mode (meaning the reactant mixtures were deposited simultaneously from separate vacuum lines) onto a KBr spectrometer window. In order to visualize only formic acid bands associated with complex formation, the formic acid/argon mixture was prepared at a concentration of about 1/20 of that of pyridine/argon. This ensured that every formic acid molecule was incorporated into a pyridine-formic acid complex and that no formic acid parent peaks were present in the codeposition spectrum.

Computational Methods

Ab initio calculations were performed on the Gaussian-03 suite for Mac OS X.[17] Density functional theory (DFT) methods have proven to provide excellent results for many chemical systems. The B3LYP level of theory allows for the timely and accurate determination of the strength of a hydrogen bonding interaction. For all calculations, the all-electron 6-311G+G(d,p) basis set, which includes a set of p- and d-functions, were used.[18] Vibrational frequencies were calculated at this level of theory, and the zero-point corrected energies (ZPCE) were obtained. The binding energy was calculated with the ZPCE energies using Equation 2

$$\Delta E = (E_A + E_B) - E_{AB} \tag{2}$$

where AB indicates the complex, A and B the separated molecules.

Experimental Results

Blank experiments were first performed for formic acid, pyridine, and 1% PVP thin film and the resulting spectra are in agreement with published data.[4,19–21] Careful assignment of each absorption band of the blank experiments was necessary to ensure a precise comparison between the parent and complex. The observed experimental frequencies, their assignments

and comparison to literature are provided in Table 1. Formic acid dimer peaks were present in all formic acid parent and soft landing eperients, regardless of dilution, but no formic acid parent peaks were observed in the matrix isolation spectra whatsoever.

Table 1: Formic Acid Parent Experiment

Fundamental	Present Study	Ito (2008)
ν(OH)	3546.8, 3548.3, 3550.32	3547, 3549, 3551
ν(C-H)	2951.67	2950
Dimer ν(C-H)	2940.1	2947
	2866.72	2868
	2770.57	2770, 2775
ν(C=O)	1761.7^{sh}, 1764.8, 1767.2	1765, 1767
Dimer ν(C=O)	1728.5	1729, 1730
Dimer ν(C-O)	1223^{sh}, 1227.11	1223, 1227
β(H-C-O)	1215.9	1216
	1173.3, 1179.5	
	1114.2, 1118.5	
ν(C-O)	1103.6, 1106.6	1104, 1107

Soft Landing Reaction. A formic acid/argon mixture was deposited on a single layer 1% PVP film, and several new absorption bands appeared in the infrared spectrum. After subtraction of the formic acid parent spectrum, a new, broad product absorption was evident at 3136.3 cm^{-1} (Figure 3). A second new product absorption band appeared at 1744.4 cm^{-1}, a distinct absorption from the nearby dimer C=O stretches (Figure 4). In addition, a new product band was observed at 1229.1 cm^{-1} (Figure 5). Upon annealing, the parent absorption bands at 1767.2 cm^{-1} and 3550.3 cm^{-1} both decreased in intensity. Note that in the soft landing experiments, the base modes for PVP did not shift substantially and thus are included in the background and not visible in the reported spectra.

Table 2: Experimental Infrared Shifts : Soft-Landing on 1% PVP and Matrix Isolation

Fundamental	FA-PVP Soft Landing	FA-Pyridine Matrix Isolation	Parent	$\Delta\nu$ Soft Landing	$\Delta\nu$ Matrix Isolation
Formic Acid					
ν(O-H)	3550.3, *3095.7*	*2902.3*	3550.3, 3548.3	-414.0	-648.0
ν(C=O)	1767.2, *1744.4*	*1707.4*	1767.2	-22.8	-59.8
ν(C-O)	1103.6, *1229.1*	*1203.4*	1103.6	+125.5	+100.0
Pyridine					
		3138.6	3088.1		+50.5
ν(C-H)	n.o.	3103.6^{br}	3041.5	n.o.	+62.1
		3072.6	3006.5		+66.1

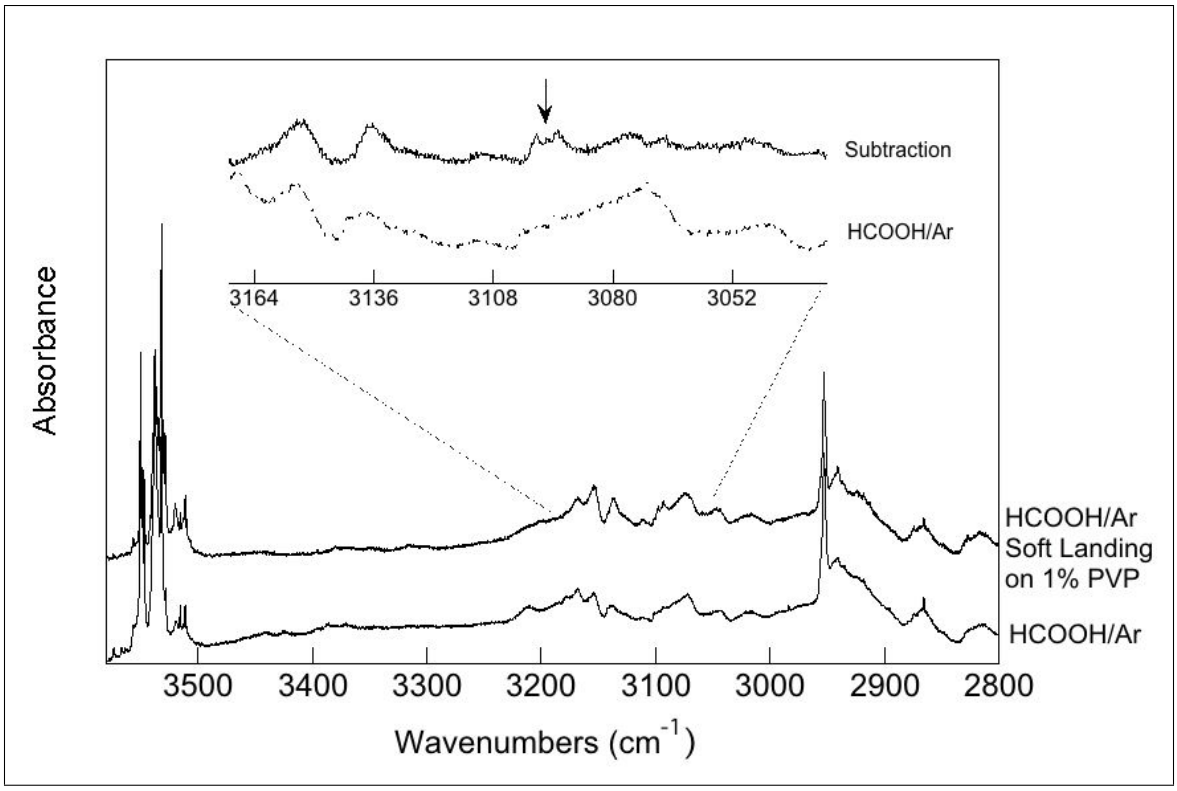

Figure 3: Formic Acid Parent and Soft Landing on 1% PVP in ν(OH) region. Inset contains a subtraction of formic acid from the soft landing experiment plotted with the formic acid parent in the region containing the shifted band. An arrow indicates the evidence of a perturbed O-H stretching mode.

Matrix Isolation Reaction Pyridine/argon and formic acid/argon mixtures were codeposited, and several new absorption bands were evident by spectral comparison; the shifted bands are summarized in Table 2. Additionally, no formic acid parent modes were observed in the codeposition experiment. Since the concentration of formic acid was far lower than that of pyridine, all formic acid molecules were incorporated into complexes, leaving none isolated to exhibit parent absorption bands. After subtracting the pyridine parent spectrum, a broad absorption band is visible at 2902.3 cm^{-1} (Figure 6). Moreover, a broad band appeared in the codeposition spectrum at 1707.4 cm^{-1} (Figure 8), and a third new absorption was visible at 1203.4 cm^{-1} (Figure 7). Also notable is the broadening and blueshift of several bands near ~3000 cm^{-1}, indicated by asterisks in Figure 6. There were no pyridine parent modes in the region of either complex band at 2902.3 cm^{-1} or 1203.4 cm^{-1}.

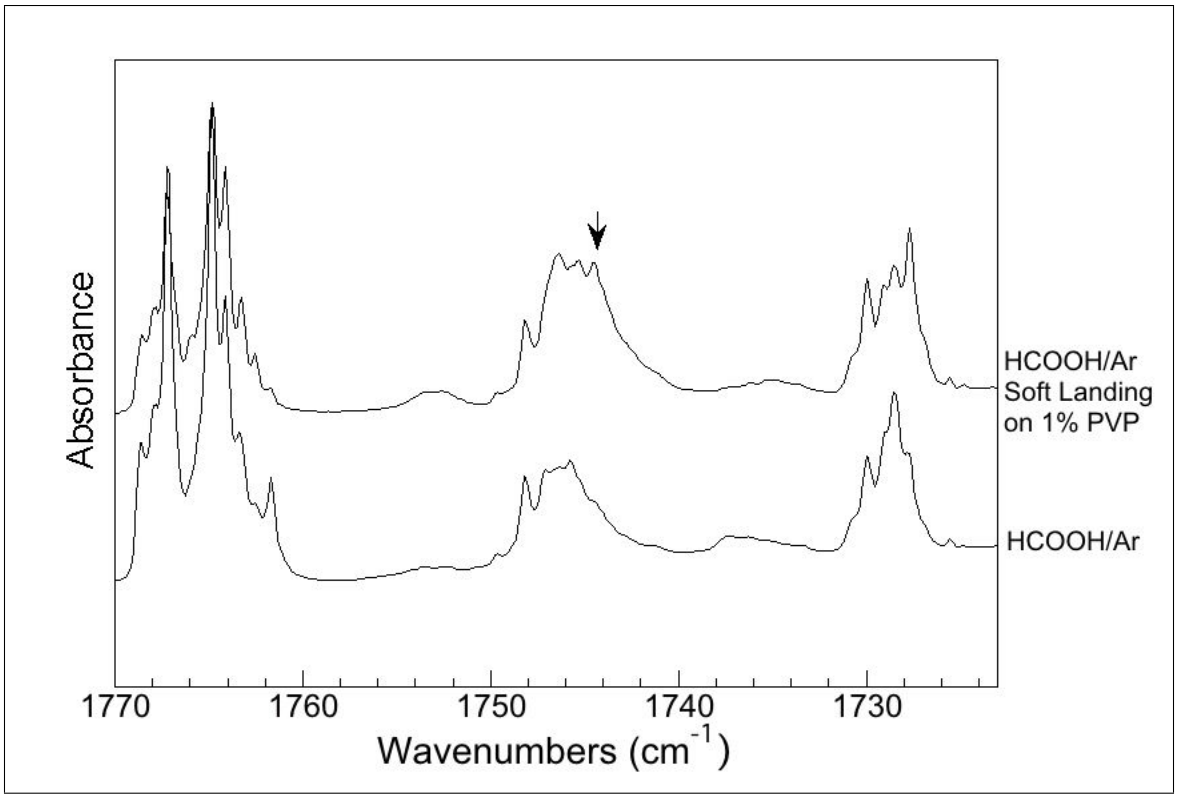

Figure 4: Formic Acid Parent and Soft Landing on 1% PVP in C=O stretching region. A new product absorption is clearly visible at 1744.4 cm^{-1}

Computational Results

Structural optimization, energy calculations, and frequency calculations were completed for formic acid, pyridine, and the pyridine-formic acid complex. The same calculations were performed for a dimer of PVP and its complex with two formic acid molecules (See Figure 2). These calculations were performed with the purpose of rationalizing any experimental observations of the complexes, and the relevant bands and their predicted shifts for each set of calculations are summarized in Table 3. All calculated frequencies were scaled down by 0.9613 as suggested by Fernandez-Berridi et al.[18] Additionally, the calculated binding energies obtained through these calculations are reported in Table 4 and compared with the value reported by Fernandez-Berridi et al. for a pyridine-formic acid system adopting the coplanar geometry.

Optimized Geometries. The DFT calculations resulted in optimal geometries for the

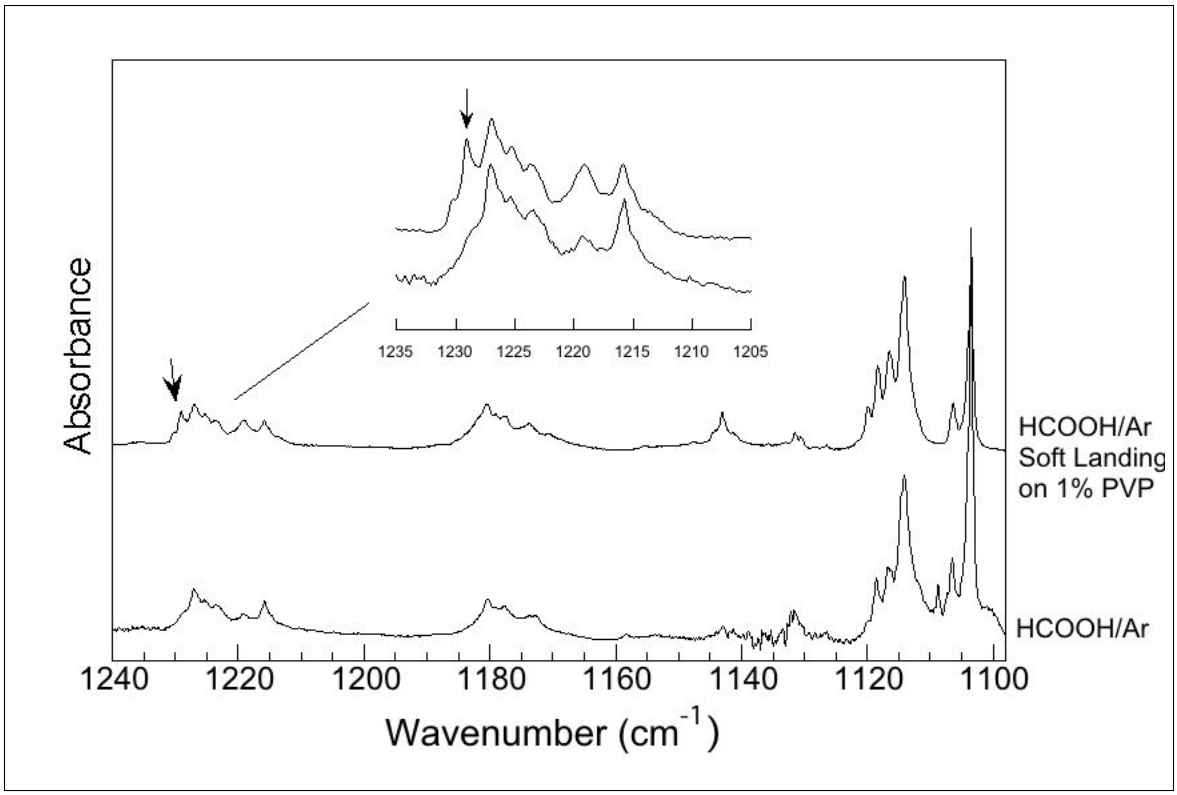

Figure 5: Formic Acid Parent and Soft Landing on 1% PVP in C-O stretching region. Inset shows both traces (top trace: soft landing, bottom trace: formic acid parent) in region containing the shifted peak at 1229 cm^{-1}, indicated by arrows

pyridine-formic acid hydrogen bond shown in Figure 9. The results from this study were compared to those reported by Fernandez-Berridi et al. for the coplanar arrangement of formic acid and pyridine.

Table 3: DFT Calculated Frequency Shifts (scaled) for Parents and Complexes

Fundamental	Pyridine	Formic	PVP Dimer	Pyr-Formic (Matrix)	PVP-Formic (Thin Film)	$\Delta\nu$ (Matrix)	$\Delta\nu$ (Thin Film)
ν(O-H)		3592.5		2812.5^{s}	2799.1	-780.0	-793.4
ν(C-H$_\alpha$)	3025.6		3027.3	3048.2	3056.5	+22.6	+29.2
ν(C=O)		1745.2		1698.8	1695.7	-46.4	-49.5
ν(C-C, C-N)	1560.2		1572.0	1574.7	1583.7	+14.5	+11.7
ν(C-O)		1082.3		1182.0	1185.2	+99.7	+102.9

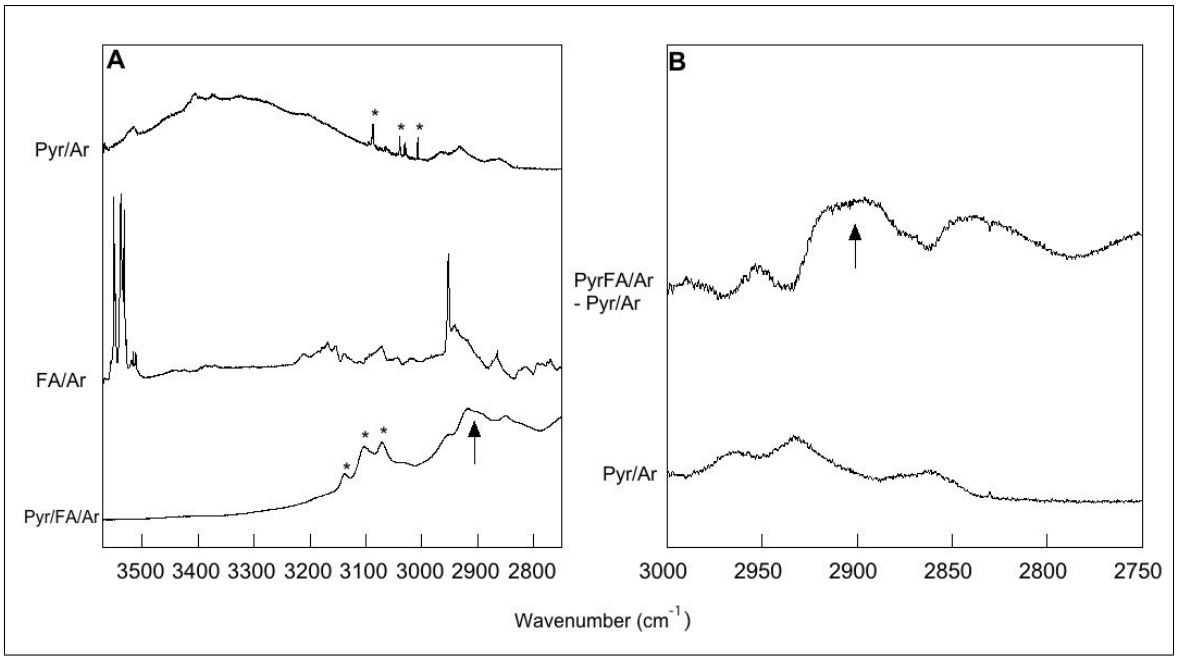

Figure 6: A) Formic acid and pyridine parent and pyridine/formic codeposition spectra in O-H/C-H stretching region. Note that no formic acid parent O-H stretch is present in the codeposition spectrum. Asterisks indicate C-H stretching modes on pyridine, arrow indicates location of shifted O-H mode (2902.3 cm^{-1}). B) Subtraction of pyridine parent from pyridine/formic codeposition displayed with pyridine parent. Arrow indicates perturbed O-H stretching band.

Table 4: Hydrogen Bond Strength for Formic Acid-Pyridine and -PVP Complexes

Complex	ΔE (Hartrees/bond)	ΔE (kcal/mol)
Pyridine-Formic Acid	0.0173	10.9
PVP-Formic Acid	0.0180	11.3
Pyridine-Formic Acid[18]		11.1

Discussion

The evidence for a hydrogen-bonding interaction between formic acid and PVP or pyridine comes from a direct comparison of the infrared spectra of isolated formic acid with those obtained during the soft landing and codeposition experiments. In particular, when formic acid was soft landed on 1% PVP thin film, ν_{OH} absorption band appeared at 3095.7 cm^{-1}, shifted about 455 cm^{-1} to the red of the parent formic acid O-H stretching mode. Shifts of similar magnitude and direction has been reported for the isolated formic acid-acetylene complex (137 cm^{-1} redshifted[22]) and for the water O-H stretch in the pyridine-water complex (201 cm^{-1} redshifted[4]). This shift is representative of a strong hydrogen-bonding interaction, though sub-

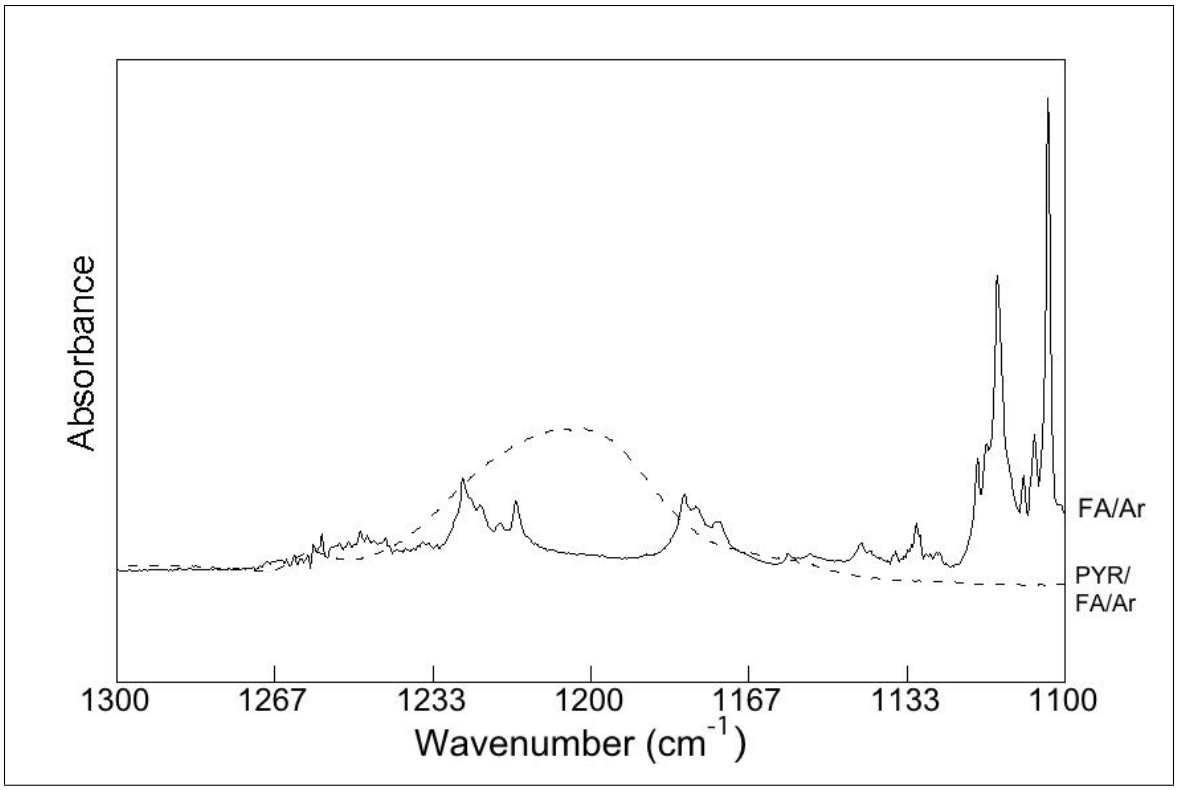

Figure 7: Formic acid Parent and pyridine/formic codeposition spectra in C-O stretching region. Formic acid parent modes are not present in the codeposition spectrum. Note the broad product band in the codeposition spectrum at 1203.4 cm^{-1}.

tracting the formic acid parent spectrum is necessary to visualize the shift because of multiple dimer bands absorbing in the same region (see Figure 3 inset). Note that when producing the subtraction spectrum, the C-H stretching mode at 2951 cm^{-1} was identified as a band that did not change in either position or intensity between the two experiments. Thus, it could easily be used to adjust the subtraction factor and elucidate the shifted band.

The complex $\nu_{C=O}$ band, red-shifted by about 23 cm^{-1}, appeared in the soft landing spectrum at 1744.4 cm^{-1} (Figure 4). At the end of deposition, this peak was noticeable only as a shoulder on the neighboring dimer bands (1746.5 cm^{-1}) but grew substantially after annealing. This behavior indicates that this absorption band is not associated with formic acid dimers but rather is evidence that the C=O stretching mode is being influenced by the formation of a hydrogen bond. The interaction of the carbonyl oxygen with an α-hydrogen of pyridine results in this perturbed $\nu_{C=O}$ band; this provides strong evidence for the coplanar geometry

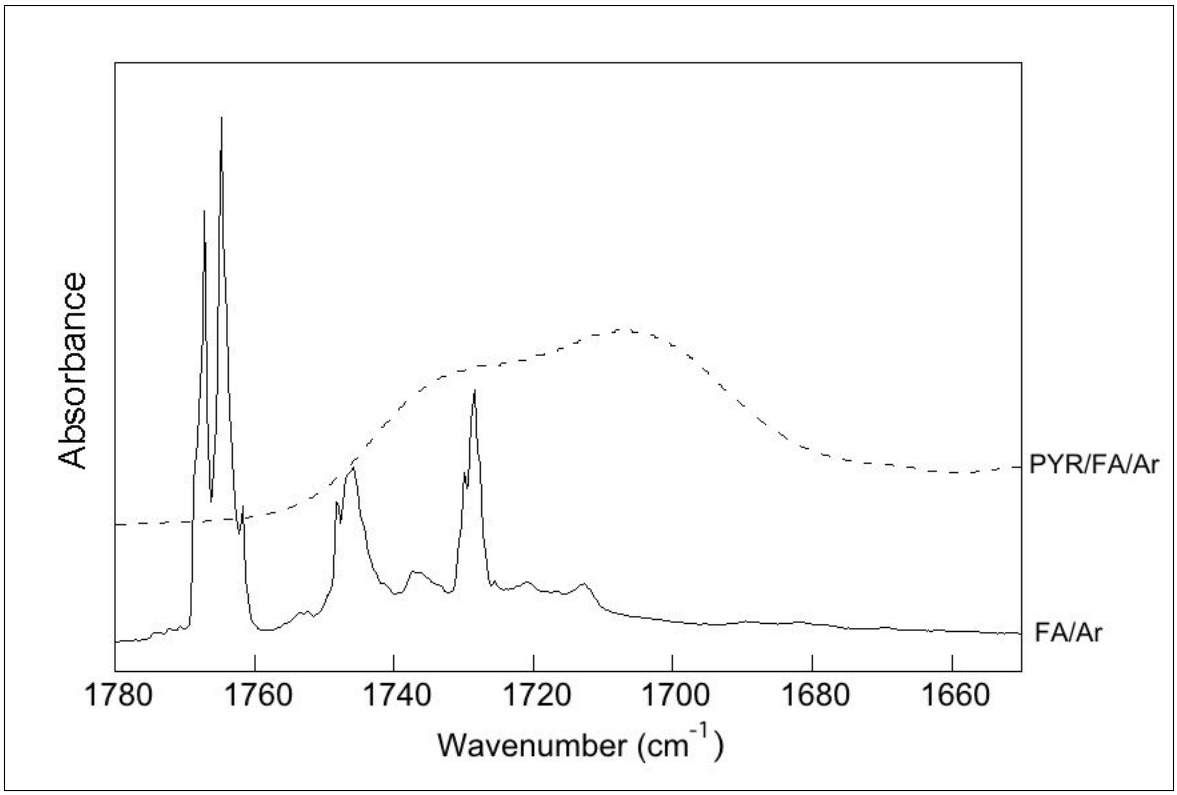

Figure 8: Formic Acid Parent and Pyridine/Formic codeposition spectra in C=O stretching region. Note the broad, red-shifted absorption band at 1707.4 cm^{-1}

depicted in Figure 1a. This weaker C=O···H-C interaction leads to a strengthening of the conventional hydrogen bond. If the formic acid molecule was rotated in a different arrangement, the carbonyl oxygen would not be subjected to direct influence by an α-hydrogen. Moreover, the red-shift of this mode suggests that it leads to the lengthening of the C=O bond, consistent with the expected interaction.[7] Thus, this shift contributes to the characterization of the hydrogen bonding interaction by providing the relative location of the carbonyl to the pyridine molecule.

The third weak product absorption band ν_{C-O} is evident in the soft landing spectrum at 1229.06 cm^{-1}, blue-shifted about 126 cm^{-1}. Similar to the complex C=O absorption, this band appeared as a shoulder of the dimer band (1227 cm^{-1}) in the spectra taken at the end of deposition and increased in intensity upon annealing. The inset of Figure 5 shows the shifted peak enlarged and denoted with an arrow. The direction of this shift is significant when placed

System	r (Å)	θ (°)
Pyridine-Formic acid	1.717	179.98
PVP-Formic acid (Site 1)	1.713	179.54
PVP-Formic acid (Site 2)	1.709	179.44
Pyridine-Formic acid[18]	1.719	180.0

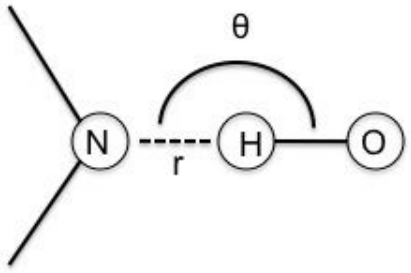

Figure 9: Optimized values for hydrogen bond length (r in Angstroms) and angle (in degrees) as calculated using B3LYP compared to those obtained by Fernandez-Berridi et al.

in the context of the hydrogen bonding interaction. While the O-H stretch occurs at a lower energy in the complex because its direction is in parallel to the hydrogen bond orientation, this C-O stretch causes the -OH group to be perturbed out of the plane of the hydrogen bond. Also, the influence of the hydrogen bond leads to an increase in the spring constant associated with the C-O bond; because the hydrogen bond angle is strongest at 180°, deviation from this conformation results in a higher energy absorption. It follows logically, therefore, that the product absorption would occur at a higher wavenumber (blue-shifted). For the soft landing of matrix-isolated formic acid on a single layer of 1% PVP film, all three shifts are in the same direction and of similar magnitude than those obtained in DFT models of the interaction, both from this study (see Table 2 and in the literature. In a theoretical study of the formic acid-pyridine hydrogen bond, the O-H stretch was red-shifted 776 cm^{-1} for the most stable conformation.[18] In the matrix isolation infrared spectra of weakly bound formic acid-acetylene reported by George et al., shifts of -137 cm^{-1}, -11 cm^{-1}, and +31 cm^{-1} were reported for the O-H, C=O, and C-O stretches of formic acid, respectively.[22] Furthermore, Pei et al. reported shifts of -443.1 cm^{-1} and -26.1 cm^{-1} for the O-H and C=O stretches of acetic acid in the theoretical study of the pyridine-acetic acid complex.[23] The experimental results indicate that formic acid molecules are strongly hydrogen bonded to pyridyl groups in a coplanar arrangement where the C=O group participates in an electrostatic interaction with a pyridyl α-hydrogen.

The matrix isolation codeposition experiments with pyridine and formic acid provided corroborating information for the shifted O-H, C=O, and C-O stretches. Spectral subtraction

reveals a growth at 2902.3 cm^{-1} that does not correspond to any pyridine or formic acid modes (Figure 6B). Since no parent formic acid modes are evident in this codeposition and the shift experienced is comparable both in magnitude and direction to the DFT calculations, this mode is a perturbed formic acid O-H stretching mode, representing a red shift of 648.0 cm^{-1}. A strong band appeared at 1707.4 cm^{-1}, representing a product C=O stretching mode red shifted by 59.8 cm^{-1}. The greater magnitude of this shift suggests that the coplanar geometry leading to the perturbed C=O stretching mode is more prevalent in matrix isolation experiments. The new, broad band occurring at 1203.4 cm^{-1} represents a blue-shirt of 100.0 cm^{-1} from the unmodified C-O stretching mode, indicating that this vibration requires a higher energy absorption to occur as predicted by theoretical calculations. This further supports the results obtained in the theoretical calculations as well as in the soft landing experiments on PVP thin film. A red-shift of 14.5 cm^{-1} was predicted by the theoretical calculations in this study of the pyridine ring stretching and bending mode at 1560.2 cm^{-1}. The soft landing experiments did not exhibit this product band because the absorbance was far lower than the formic acid bands previously described; all unshifted PVP bands are included in the background, and a shifted product band was not observed. Moreover, this band's intensity was too weak in the matrix isolation spectrum to confirm the shift predicted by theory.

The pyridine C-H absorption bands (marked by asterisks in Figure 6A) appear in the matrix isolation experiments as broad, blue-shifted bands (see Table 2. The complexation of a hydrogen bond at the nitrogen results in electron density being drawn away from carbons within the pyridine ring. Also, the shifted C=O stretching mode indicates an interaction between the carbonyl oxygen and an $\alpha-$hydrogen. Both of these forces result in the lengthening of one or more of the C-H bonds on the pyridine ring, confirming the red-shift observed by these bands. In addition, blueshifts of similar magnitudes were predicted by DFT calculations (see Table 3). Thus, the broadening and red-shifting of these modes is consistent with the expected geometry of the complex. The location of these C-H modes complicates the assignment of the perturbed O-H mode, an issue not encountered as a part of the soft landing experiment because unshifted

PVP base modes were included in initial background spectra. This could not be accomplished in a standard matrix experiment because backgrounds were taken before starting the deposition of either reactant mixture meaning that all infrared modes of both parent molecules in addition to complex bands were present in all spectra. This represents an additional benefit of the soft landing technique afforded when modes indicative of hydrogen bonding are localized on the isolated reactant and not in the thin film.

The soft landing and matrix isolation techniques both have advantages and disadvantages for the study of hydrogen bonding. In a matrix experiment, more and more complexes are formed as the deposition of both reactants continues. Thus, deposition can be continued until enough molecules are present to visualize a perturbed mode. Conversely, in a soft landing experiment, hydrogen bonding sites are limited, and continued deposition of the single reactant only results in stronger parent absorptions, so higher reactant concentration is necessary which may result in dimer formation (as is clearly the case with formic acid). However, the deposition times associated with soft landing experiments are about 1/3 as long as traditional matrix isolation experiments, a clearly advantageous property when multiple systems are being explored. An additional benefit of this particular soft landing study is avoiding the frequent handling of the highly toxic and flammable liquid pyridine.

The binding energy values for the theoretical hydrogen bonded complexes in the coplanar conformation are in strong agreement with those reported by Fernandez-Berridi et al.[18] These values should be compared with those reported for other known strong hydrogen bonds: Pei et al. reported a calculated binding energy of 18.7 kcal/mol for the pyridine-acetic acid hydrogen bond,[23] and Čeponkus et al. provided a binding energy of 7.8 kcal/mol for the formic acid-water complex.[24] This further supports the experimental infrared results that suggest the isolated formic acid molecules form similar structures with both isolated pyridine and poly(4-vinylpyridine) thin films. However, this calculation was performed using a PVP dimer due to time constraints; each B3LYP calculation for the PVP-formic acid complex took nearly 5 days to complete. Each additional monomer unit would drastically increase the calculation time, and

such a calculation would require exorbitant amounts of memory. While these energetic calculations agree well with literature values, the actual polymer chains used in this experiment averaged 1500 monomers in length. The steric hindrance associated with these long chains has the potential to drastically reduce the binding energy of hydrogen bonding interactions by preventing the isolated formic acid molecules from adopting the coplanar, hydrogen-bonded arrangement.

Conclusions

This study presents one of the first examples of a thin film of polymer with hydrogen bonding acceptors to be characterized using the soft-landing technique and FT-IR absorbance. This particular complex, pyridine-formic acid, was selected as a prototype system for several reasons: the interaction is a strong hydrogen bond with large shifts associated with hydrogen bond formation; poly(4-vinylpyridine) has been previously studied for its hydrogen-bonding properties and is known to form multilayer films with poly(acrylic acid); crucial spectral comparison using the matrix isolation and soft landing techniques were necessary to fully characterize this complex; successful comparison of shifted modes in the matrix isolation and soft landing spectra represents a novel method of studying hydrogen bonding that can be applied to many other systems.

Experimental soft landing spectra contain three new formic acid bands which are indicative of perturbed O-H, C=O, and C-O stretching modes. All three modes are discernible in the traditional matrix isolation experiment with pyridine and formic acid and agree with the soft landing values in both direction and magnitude. In addition to the spectral evidence for the hydrogen bonding of formic acid and PVP, calculations were performed to confirm the shifts were indeed associated with hydrogen bonding activity, and the binding energies obtained from these calculations agrees strongly with literature values. Additionally, based on the shifting C=O stretching mode, it is clear that the coplanar arrangement of the formic acid with pyridine or PVP is adopted in both the soft landing and matrix isolation experiments.

This model study represents an important step by demonstrating a novel application of the matrix isolation technique and has far-reaching implications both in physical chemistry and other fields. Now that it has been shown that soft landing on a hydrogen-bonding thin film produces comparable changes in infrared spectra to a related matrix isolated system, many other systems are now viable candidates for similar studies. Future work will involve soft landing of isolated base molecules poly(acrylic acid) to further investigate the interlayer attractions between PVP and PAA. Furthermore, multiple bilayers of PVP/PAA could be deposited in order to investigate any changes in hydrogen bonding activity resulting from this introduction of interlayer forces. Additionally, poly(2-vinylpyridine), an isomer of the polymer explored in this study, will be examined to determine whether the steric hindrance associated with the location of the nitrogen leads to a difference in the structure and energetics of the resulting complex. Many systems in the field of nanochemistry rely heavily on hydrogen bonding interactions, and soft landing of isolated molecules on thin films will prove to be a valuable tool for investigating such systems.

Acknowledgments

The author gratefully recognizes the support of the Dickinson College Chemistry Department for support, Alejo Lifschitz for assistance in data collection and reagent purification, Lucky Challyandra for assistance with NMR analysis of dry formic acid.

References

(1) Dunkin, I. R. *Matrix-Isolation Techniques. A Practical Approach*; Oxford University Press: New York, 1998.

(2) Lucena, J. R.; Sharma, A.; Reva, I. D.; Araújo, R. M. C. U.; Ventura, E.; do Monte, S. A.; Braga, C. F.; Ramos, M. N.; Fausto, R. *J. Phys. Chem. A* **2008**, *112*, 11641–11648.

(3) Clay, M.; Ault, B. S. *J. Phys. Chem. A* **2010**, *114*, 2799–2805.

(4) Destexhe, A.; Smets, J.; Adamowicz, L.; Maes, G. *J. Phys. Chem.* **1994**, *98*, 1506–1514.

(5) Bedell, B. L.; Goldfarb, L.; Mysak, E. R.; Samet, C.; Maynard, A. *J. Phys. Chem. A* **1999**, *103*, 4572–4579.

(6) Baker, A. B.; Samet, C.; Lyon, J. T.; Andrews, L. *J. Phys. Chem. A* **2005**, *109*, 8280–8289.

(7) Scheiner, S.; Kar, T. *J. Phys. Chem. A* **2002**, *106*, 1784–1789.

(8) Khriachtchev, L. *J. Mol. Struct.* **2008**, *880*, 14–22.

(9) Hao, E.; Lian, T. *Langmuir* **2000**, *16*, 7879–7881.

(10) Fujimori, K.; Trainor, G. T.; Costigan, M. J. *J. Polym. Sci., Polym. Chem. Ed.* **1984**, *22*, 2479.

(11) Inai, Y.; Kato, S.; Hirabayashi, T.; Yokota, K. *J. Polym. Sci., Part A: Polym. Chem.* **1996**, *34*, 2341.

(12) Oyama, H.; Nakajima, T. *J. Polym. Sci., Polym. Chem. Ed.* **1983**, *21*, 2897.

(13) Nagaoka, S.; Matsumoto, T.; Ikemoto, K.; Mitsui, M.; Nakajima, A. *J. Am. Chem. Soc.* **2007**, *129*, 1528–1529.

(14) Armarego, W. L. F.; Chai, C. L. L. *Purification of Laboratory Chemicals, Sixth Edition*; Butterworth-Heinemann: Burlington, MA, 2009.

(15) Malynych, S.; Luzinov, I.; Chumanov, G. *J. Phys. Chem. B* **2002**, *106*, 1280–1285.

(16) Cesteros, L. C.; Isasi, J. R.; Katime, I. *Macromolecules* **1993**, *26*, 7256–7262.

(17) Frisch, M. J. et al. GAUSSIAN 03, Revision E.01, Gaussian, Inc.: Wallingford, CT, 2004.

(18) Fernandez-Berridi, M. J.; Iruin, J. J.; Irusta, L.; Mercero, J. M.; Ugalde, J. M. *J. Phys. Chem. A* **2002**, *106*, 4187–4191.

(19) Ito, F. *J. Chem. Phys.* **2008**, *128*, 114310.

(20) Sánchez-García, E.; George, L.; Montero, L. A.; Sander, W. *J. Phys. Chem. A* **2004**, *108*, 11846–11854.

(21) Szczepaniak, K.; Chabrier, P.; Person, W. B.; Del Bene, J. E. *J. Mol. Struct.* **1997**, *436-437*, 367–386.

(22) George, L.; Sanchez-Garcia, E.; Sander, W. *J. Phys. Chem. A* **2003**, *107*, 6850–6858.

(23) Pei, K.; Li, Y.; Li, H. *J. Mol. Struct.* **2003**, *660*, 113–118.

(24) Čeponkus, J.; Leščiūtė, D.; Čepulinskaitė, D.; Pučetaitė, M.; Šablinskas, V. *Lithuanian J. Phys.* **2009**, *49*, 53–62.